Biochimica et Biophysica Acta 1854 (2015) 827–833

Contents lists available at ScienceDirect

Biochimica et Biophysica Acta

journal homepage: www.elsevier.com/locate/bbapap

Interaction proteomics of canonical Caspr2 (CNTNAP2) reveals the presence of two Caspr2 isoforms with overlapping interactomes ☆

Ning Chen [a,b], Frank Koopmans [b], Aaron Gordon [c], Iryna Paliukhovich [a], Remco V. Klaassen [a], Roel C. van der Schors [a], Elior Peles [c], Matthijs Verhage [b], August B. Smit [a,1], Ka Wan Li [a,*,1]

[a] Department of Molecular and Cellular Neurobiology, Center for Neurogenomics and Cognitive Research, Neuroscience Campus Amsterdam, VU University, De Boelelaan 1085, Amsterdam 1081 HV, The Netherlands
[b] Department of Functional Genomics, Center for Neurogenomics and Cognitive Research, Neuroscience Campus Amsterdam, VU University, De Boelelaan 1085, Amsterdam 1081 HV, The Netherlands
[c] Department of Molecular Cell Biology, The Weizmann Institute of Science, Rehovot 76100, Israel

ARTICLE INFO

Article history:
Received 18 September 2014
Received in revised form 31 January 2015
Accepted 11 February 2015
Available online 21 February 2015

Keywords:
Autism
Caspr2
Interaction proteomics
Mouse model
Brain

ABSTRACT

Autism is a human developmental brain disorder characterized by impaired social interaction and communication. Contactin-associated protein-like 2 (Caspr2, CNTNAP2) is a known genetic risk factor of autism. However, how this protein might contribute to pathology is unclear. In this study, we demonstrate that Caspr2 is abundantly present in lipid raft and in the synaptic membrane but is highly depleted in the postsynaptic density. The Caspr2 protein level in hippocampus is present at a constant level during synapse formation and myelination from P0 to P84. Interaction proteomics revealed the interactors of Caspr2, including CNTN2, KCNAs, members of the ADAM family (ADAM22, ADAM23 and ADAM11), members of LGI family and MAGUKs (DLGs and MPPs). Interestingly, a short form of Caspr2 was detected, which lacks most of the extracellular domains, however, is still associated with ADAM22 and to a lesser extent LGI1 and Kv1 channels. The comprehensive Caspr2 interactome revealed here might aid in understanding the molecular mechanisms underlying autism. This article is part of a Special Issue titled *Neuroproteomics: Applications in Neuroscience and Neurology*.

1. Introduction

Autism spectrum disorder (ASD) is the most prevalent developmental brain disorder in children. The diagnosis of ASD is based on abnormalities in social interaction, impairments in language development and communication and occurrence of repetitive or stereotyped behaviors [1]. In addition, many ASD patients have seizures and display intellectual disability. The cause, or causes, of ASD are largely unknown. The high heritability of autism was demonstrated convincingly by concordance rates in genetic studies in families and twins [2,3]. Considerable symptom heterogeneity in the autism spectrum exists, which may be indicative of the underlying genetic complexity of the disorder. Currently, over 100 ASD-genes have been reported by genetic analysis [4,5]. In particular, mutations in Shank, Caspr2, Neurexin and Cadherin, cell adhesion molecules and components of the synapse have been linked to ASD [5–7]. This supports the hypothesis that synaptic dysfunction is an underlying cause, at least in part, of the observed ASD behavioral phenotypes.

Recent behavioral and physiological studies revealed the prominent role of contactin-associated protein-like 2 (Caspr2, CNTNAP2) in ASD [8–10]. In particular, Caspr2 knockout mice exhibited behavioral abnormalities that mimic some of the core features of ASD [8,11]. At the cellular level, knockout mice showed neuronal migration abnormalities, reduced numbers of interneurons and abnormal neuronal network activity [8]. Similar alterations were reproduced independently by the knockdown of Caspr2 transcripts in a cortical neuron culture in vitro, which exhibited impaired synapse formation and neural network assembly leading to a global decrease of synaptic transmission [10]. How mutations at the Caspr2 locus and/or reduction of Caspr2 expression cause ASD remains largely unclear.

Caspr2 is a single pass transmembrane cell adhesion protein. The extracellular region of Caspr2 is composed of several domains common to cell adhesion molecules, including laminin G, EGF repeats and discoidin-like domains. Caspr2 interacts with Contactin 2 (CNTN2) extracellularly, forming a neuron–glia cell adhesion complex [12]. The short intracellular region of Caspr2 contains a band 4.1 binding domain and a carboxy-terminal PDZ-binding motif, which might be involved in the clustering of voltage-gated potassium channels 1 (Kv1, KCNA) in myelinated axon membranes [13]. This clustering of Kv1 channels in myelinated axon membranes, permits a rapid and efficient propagation of action potentials at the juxta-paranodal membrane of the nodes of

☆ This article is part of a Special Issue titled Neuroproteomics: Applications in Neuroscience and Neurology.

* Corresponding author. Tel.: +31 20 5987107; fax: +31 20 5989281.
E-mail address: k.w.li@vu.nl (K.W. Li).

[1] These authors have equal contribution.

http://dx.doi.org/10.1016/j.bbapap.2015.02.008
1570-9639/

Ranvier [12]. Besides, Caspr2 has been shown to associate with Kv1 channels in the distal region of the axon initial segment of pyramidal neurons, which is crucial for controlling action potential initiation and neural activity [14]. Caspr2 has also been demonstrated in the synaptic plasma membrane of brain lysates [15].

To improve understanding of Caspr2 function, we examined the subcellular localization of Caspr2 by biochemical fractionation and the developmental expression pattern of Caspr2. We then characterized the Caspr2 protein complex in two preparations, namely, an extract of synapse-enriched fraction of the hippocampus and an extract from whole cortex, in wild-type and Caspr2 knockout mice. In addition to the previously reported Caspr2 interactors, we detected a Caspr2 isoform 2. In the Caspr2 knockout mice, the short Caspr2 isoform 2, lacking most of the extracellular domains, is still present and is capable of interacting with a subset of the Caspr2 long isoform interactors.

2. Materials and methods

2.1. Subcellular fractionation of hippocampal lysate

Mature C57Bl6 mice brains were taken at postnatal days P56-P70, and hippocampi were dissected on ice [16] and stored at −80 °C for further use. Frozen hippocampi were homogenized in homogenization buffer (320 mM sucrose, 5 mM HEPES (pH 7.4) and a protease inhibitor mixture(Roche Applied Science)) using a dounce homogenizer on ice, and centrifuged at 1,000 ×*g*. The supernatant was further centrifuged at 16,000 ×*g* for 20 min to obtain the pellet as P2 fraction. The supernatant was centrifuged at 85,000 ×*g* for 2 h to obtain the pellet as microsome fraction. The P2 fraction was centrifuged at 85,000 ×*g* for 2 h in a sucrose step gradient to obtain the synaptosome fraction at the 0.85 M/1.2 M sucrose interface. Synaptosomes were lysed in hypotonic solution containing 5 mM HEPES (pH 7.4), and the resulting synaptic membrane fraction was recovered by centrifugation using the sucrose gradient as stated above. To obtain postsynaptic density (PSD) and lipid raft, the P2 and microsome fractions were pooled and stirred for 30 min on ice in 50 mM HEPES (pH 7.4) containing 1% Triton X-100. The sample was loaded on top of a sucrose gradient consisting of 0.32 M, 1.0 M, 1.5 M and 2.0 M sucrose and centrifuged at 85,000×*g* for 2 h. The interface between 1.5 M and 2.0 M was collected as PSD and the interface between the input and 0.32 M as lipid raft.

2.2. Affinity isolation of the Caspr2 protein complex

Hippocampi and cortices were dissected from mature C57Bl6 wild-type and Caspr2 knockout mice [11] and stored at −80 °C. For the analysis of Caspr2 interactome from hippocampus, we followed the protocol as described previously [17]. In short, the P2 and microsome (P2 + M) fraction was extracted in a buffer (150 mM NaCl, 50 mM HEPES (pH 7.4) containing 1% Triton X-100 and the protease inhibitor mixture) at 4 °C. The extract was incubated with primary antibody to the bait protein on a rotator at 4 °C overnight. On the second day, protein A/G PLUS-agarose beads (Santa Cruz) were added and incubated at 4 °C for 1 h. Bound proteins were eluted from the beads for subsequent analysis. The quantities of the materials and reagents were 5 mg P2 + M fraction, 10 μg antibody and 50 μl slurry of protein A/G PLUS-agarose beads for a typical SDS–PAGE/MS experiment.

In the second experiment, we used the total cortical extract as input. A single cortex was directly homogenized in 5 mL buffer containing 150 mM NaCl, 50 mM HEPES (pH 7.4), 0.5% *n*-dodecyl β-D-maltoside (DDM) and the protease inhibitor mixture at 4 °C. The extract was incubated with antibody and further analyzed by SDS–PAGE/MS as described above.

Polyclonal antibody against Caspr2 (catalog number A01426) and its antigen peptide were purchased from Genscript; monoclonal antibodies against ADAM22 (catalog number 75–083) and DLG4 (catalog number 75–028) and Kv1.1 (catalog number 75–105) were purchased from Neuromab.

2.3. SDS–PAGE separation of IP samples and in-gel trypsin digestion

The protein A/G beads with Caspr2 antibody and the bound Caspr2 protein complexes were mixed with 14 μl 2× SDS sample buffer and heated to 98 °C for 5 min. To block cysteine residues, 5 μl 30% acrylamide was added and incubated at room temperature for 30 min [18]. Proteins were then resolved on a 10% SDS–polyacrylamide gel and stained with colloidal Coomassie blue G-250 for 30 min. The gel lane of each sample was cut into five pieces. Each was chopped into smaller pieces using a scalpel and transferred to an Eppendorf tube. The gel pieces were destained with 50% acetonitrile in 50 mM ammonium bicarbonate, dehydrated in 100% acetonitrile and rehydrated in 50 mM ammonium bicarbonate. The destaining cycle was repeated once. After dehydration in 100% acetonitrile and dried in a speedvac, the gel pieces were incubated with trypsin solution containing 10 μg/mL trypsin (sequence grade; Promega, Madison, USA) in 50 mM ammonium bicarbonate overnight at 37 °C. Peptides from the gel pieces were extracted twice with 200 μL 50% acetonitrile in 0.1% Trifluoroacetic acid, dried in a SpeedVac and stored at −20 °C for future use.

2.4. HPLC-MS/MS analysis

Peptides were re-dissolved in 20 μL 0.1% acetic acid and injected into an LTQ-Orbitrap mass spectrometer (Thermo Electron, San Jose, CA, USA) equipped with an HPLC system (Eksigent). Samples were first trapped on a 5 mm Pepmap 100 C18 (Dionex) column (300 μm ID, 5 μm particle size) and then analyzed on a 200 mm Alltima C18 home-made column (100 μm ID, 3 μm particle size). Separation was achieved by using a mobile phase from 5% acetonitrile, 94.9% H_2O, 0.1% acetic acid (solvent A) and 95% acetonitrile, 4.9% H_2O and 0.1% acetic acid (solvent B), and the linear gradient was from 5% to 40% solvent B for 40 min at a flow rate of 400 nL/min. The LTQ-Orbitrap mass spectrometer was

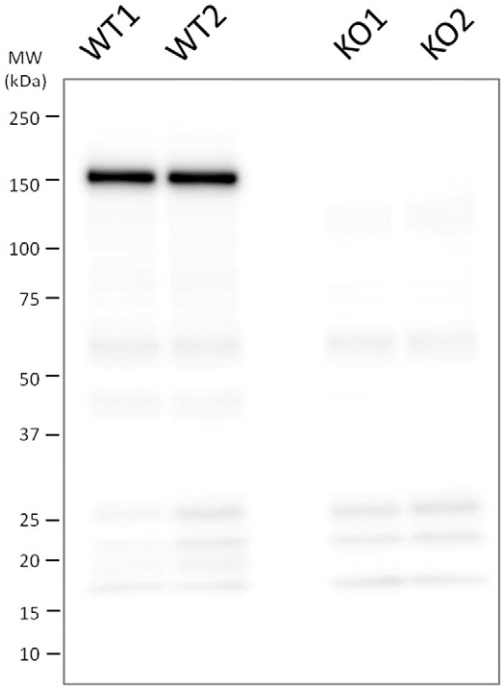

Fig. 1. Western blotting of Caspr2 antibody. Fifteen micrograms of DDM extracts of cortices from two wild-type mice (WT1 and 2) and two knockout mice (KO1 and 2) were separated on a 10% SDS–PAGE, electro-blotted on PVDF membrane and immunostained with anti-Caspr2 antibody. A major immunoreactive band is present around 150 kDa corresponding to the expected mass of Caspr2.

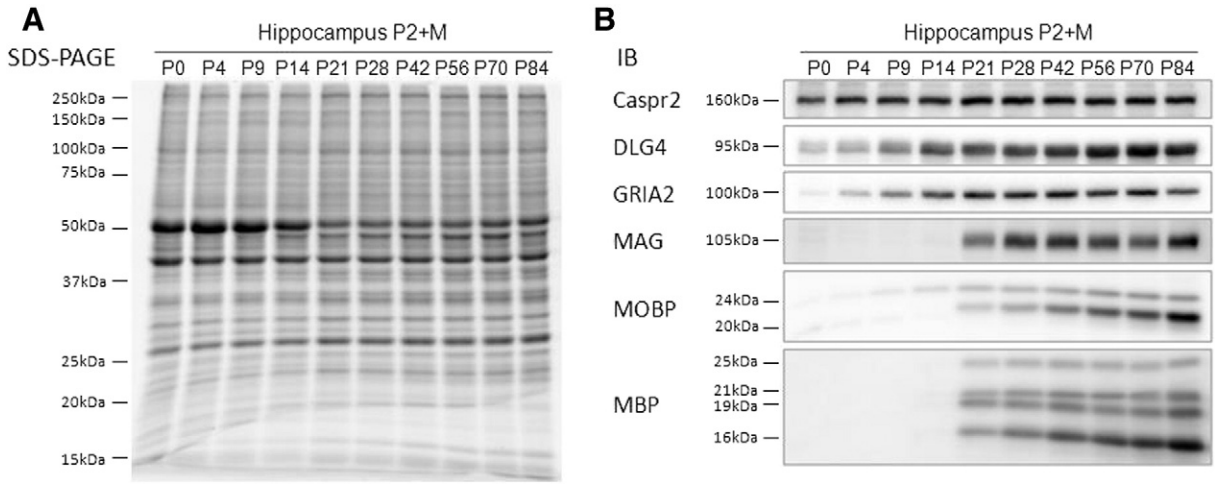

Fig. 2. Caspr2 expression during brain development. (A) Protein input of the hippocampus P2 + M from brain developmental series for immunoblotting and visualized on homemade stain-free SDS–PAGE gel with Gel Doc EZ system (Bio-Rad). (B) Immunoblotting analysis of Caspr2, synaptic proteins and myelin proteins. Caspr2 is detected in hippocampus over all ages of mice, with a slight increase in level from P0 till P21, after which expression is stable. Synaptic proteins GRIA2 and DLG4 are expressed increasingly after birth and stabilize around P21, whereas myelin proteins MAG, MOBP and MBP are expressed from P21 and get to full expression only at P84.

operated in the data-dependent mode, in which one full-scan survey MS experiment (m/z range from 330 to 2000) was followed by MS/MS experiments on the five most abundant ions.

2.5. Data analysis

The mass spectra were searched against the Uniprot proteomics database (version 2013-01-06) with MaxQuant software (version 1.5). The mass tolerances in MS and MS/MS were set to 6 ppm and 0.5 Da, respectively. Trypsin was designated as the protease, and up to two missed cleavages were allowed. Cysteine alkyation with acrylamide was set as fixed modification; methionine oxidation and protein N-terminal acetylation were set as variable modifications. False discovery rates of both peptides and proteins were set within 0.01. The valid protein hits should contain at least one unique peptide. For intensity-based absolute quantification (iBAQ), the summed MS intensity of all assigned peptides for each protein was divided by the number of theoretically observable peptides. Only unique peptides were used for identification and quantitation.

2.6. Immunoblotting

Samples were separated by homemade stain-free SDS–PAGE gels containing 0.5% 2,2,2-trichloroethanol (Sigma-Aldrich) or Criterion™ TGX stain-free™ precast gels (Bio-Rad), scanned with Gel Doc EZ system (Bio-Rad) and then transferred to PVDF membranes (Bio-Rad) at 40 V at 4 °C overnight. After blocking with 5% non-fat dried milk in Tris-buffered saline Tween-20 (TBST) (28 mM Tris, 136.7 mM NaCl,

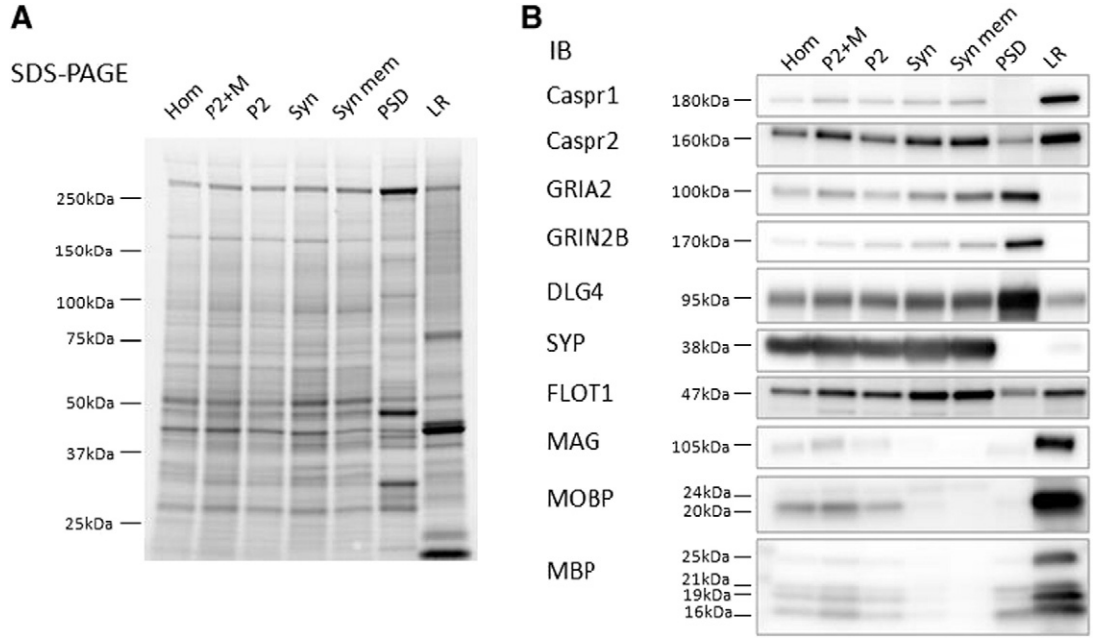

Fig. 3. Caspr2 levels in different subcellular fractions of hippocampal lysates. (A) Protein input of the subfraction samples for immunoblotting, separated on Criterion™ TGX stain-free™ precast gels (Bio-Rad) and scanned with Gel Doc EZ system (Bio-Rad). Hom: homogenate; P2 + M: pellet 2 and microsome; P2: pellet 2; Syn: synaptosome; Syn mem: synaptic membrane; PSD: Triton X-100 insoluble postsynaptic density fraction; LR: Triton X-100 insoluble lipid raft fraction. (B) Immunoblot analysis of Caspr2, synaptic proteins and myelin proteins. Compared to Caspr1 (CNTNAP1), Caspr2 is abundant in the synaptic membrane fraction and in the myelin-associated fractions. GRIA2, GRIN2B and DLG4 are used as markers for the post-synaptic compartment; SYP and FLOT1 are markers of the pre-synaptic terminal and lipid raft, respectively; MAG, MOBP and MBP were taken as markers of the myelin-associated fractions.

Table 1
Proteins identified from the IPs with anti-Caspr2 antibody from hippocampal P2 + microsome fraction.

Gene name	Protein name	Experiment 1				Experiment 2		
		KO1	KO2	WT1	WT2	WT1	WT2	WT3
CNTNAP2 (isoform 1)	Isoform 1 of contactin-associated protein-like 2 (Caspr2 isoform 1)			8.6E+07	8.7E+07	4.3E+07	3.5E+07	4.1E+07
CNTNAP2 (isoform 2)	Isoform 2 of contactin-associated protein-like 2 (Caspr2 isoform 2)	6.5E+05	2.4E+06	1.2E+07	1.8E+07	1.7E+07	1.8E+07	1.7E+07
CNTN2	Contactin-2			2.2E+06	2.4E+06	1.1E+06	8.7E+05	9.8E+05
LGI1	Leucine-rich glioma-inactivated protein 1	2.1E+04	8.5E+04	1.4E+06	8.2E+05	1.1E+05	1.3E+05	1.5E+05
KCNAB2	Voltage-gated potassium channel subunit beta-2	1.7E+05		9.4E+05	1.0E+06	4.2E+05	1.4E+05	4.4E+05
ADAM22	Disintegrin and metalloproteinase domain-containing protein 22	1.2E+04	1.8E+04	4.9E+05	2.2E+05	1.1E+05	6.5E+04	7.5E+04
ADAM23	Disintegrin and metalloproteinase domain-containing protein 23			3.2E+05	2.3E+05	3.3E+04	7.2E+04	7.7E+04
MPP3	MAGUK p55 subfamily member 3			1.6E+05	1.8E+05	7.4E+03		
CLU	Clusterin			1.5E+05	1.7E+05	2.5E+04		
DLG4	Disks large homolog 4			1.1E+05	5.3E+04	1.1E+04	1.5E+04	1.9E+04
KCNA2	Potassium voltage-gated channel subfamily A member 2 (Kv1.2)			8.1E+04	6.1E+04	3.9E+04		2.2E+04
CKMT1	Creatine kinase U-type, mitochondrial			7.5E+04	1.8E+04	1.3E+04		
ADAM11	Disintegrin and metalloproteinase domain-containing protein 11			6.9E+04	9.8E+04	8.9E+03	1.3E+04	1.1E+04
DLG1	Disks large homolog 1			2.9E+04	8.8E+04			3.9E+03

Multiple replicates were done in two batches. The first experiment includes IPs from two knockout (KO 1 and 2) and two wild-type samples (WT 1 and 2), and the second experiment includes three IP replicates from wild-type samples (WT 1, 2 and 3). The iBAQ values of the identified proteins are shown, corresponding to their protein abundance (descending values). When no values are depicted, signal was below detection limit.

0.05% Tween-20, pH 7.4) for 4 h, membranes were incubated with the primary antibody with 3% non-fat dried milk in TBST at 4 °C overnight, followed by the secondary antibody for 1 h at room temperature. Target proteins were detected by ECL (Pierce) on the scanner (LICOR).

In addition to the antibodies described in the affinity isolation of the Caspr2 protein complex, multiple antibodies were used for immunoblotting, including monoclonal antibodies against Caspr1 (catalog number 75–001), AMPA-selective glutamate receptor 2 (GRIA2, catalog number 75–002) and NMDA receptor 2b (GRIN2B, catalog number 75–097) from Neuromab; myelin basic protein (MBP) polyclonal antibody (catalog number ab91405) and Myelin oligodendrocytebasic protein (MOBP) monoclonal antibody (catalog number ab7349) from Abcam; myelin-associated glycoprotein (MAG) monoclonal antibody (catalog number sc9544) from Santa Cruz; synaptophysin (SYP) polyclonal antibody (catalog number A01307) from Genscript; and Flotillin 1 (FLOT1) polyclonal antibody made against peptide sequence CKLPQVAEEISGPLT.

3. Results

The success of the experiments is critically dependent on the quality of the Caspr2 antibody. We performed Western blotting analysis on the cortical extracts from Caspr2 knockout and wild-type mice. Fig. 1 shows the intense immunostained band at 150 kDa, corresponding to the mass of Caspr2, in wild-type samples, which is absent in the knockout samples.

3.1. Caspr2 protein level is constant through brain development

Caspr2 is involved in the neuron-oligodendrocyte interaction and clustering of Kv1 channels in myelinated axons. Recently, Caspr2 has been implicated in synapse development [10], which is a distinct physiological process and independent of myelination. We examined the Caspr2 protein level in hippocampus during synapse formation and myelination from P0 to P84 (Fig. 2). The Caspr2 protein level is fairly constant across all time points, in contrast to the postsynaptic proteins, GRIA2 and DLG4, which show a gradual increase in expression throughout adolescence and stabilize in adulthood. Myelin proteins only start to show up at P21 and reach a maximum in adulthood. Thus, Caspr2 might be involved in multiple processes with early onset in brain development and extending throughout brain development.

3.2. Caspr2 is present in lipid raft and synaptic membrane fractions

To examine the subcellular distribution of Caspr2, immunoblotting of synaptic subfractions was carried out (Fig. 3). Caspr2 is present abundantly in the lipid raft fraction. In the synaptic fractions, Caspr2 is present in P2, synaptosome and synaptic membrane but is depleted in the PSD. This suggests that the synaptic Caspr2 is present mainly outside the PSD. For comparison, typical PSD proteins, such as the glutamate receptors (GRIN2B and GRIA2) and the scaffolding protein (DLG4), are enriched in the PSD, whereas the typical myelin proteins (MAG, MOBP and MBP) are present mainly in the lipid raft. Caspr1 is highly present in lipid raft and much lower in synaptic fractions.

Based on the co-occurrence in similar subfractions, it is likely that Caspr2 and its known interactor, DLG4, form protein complex in synaptic membrane and lipid raft.

3.3. Interaction proteomics of Caspr2 reveals multiple protein complexes

Two experiments were performed using hippocampus and cortex, respectively. In the first experiment, the Caspr2 protein complex was immunoprecipitated from the hippocampus P2 + M fraction. We have performed the experiments in two batches, namely, IPs from 3 WT mice and IPs from 2 WT and 2 KO. 359 proteins were identified at least once from the 7 IPs. To reveal the true Caspr2 interactors from the background, the identification in at least 3 out of the 5 IPs from the WT samples was required, as well as a 10-fold depletion in the KO samples. This reduces the list to 14 proteins (Table 1). The known interactors CNTN2, ADAM22, LGI1, subunits of Kv1 channel and DLG4

Table 2
Reverse IPs reveal the presence of full length Caspr2 (isoform 1) in the complex.

Gene name	Protein name	ADAM22_IP1	ADAM22_IP2	DLG4_IP1	DLG4_IP2	Kv1.1_IP1	Kv1.1_IP2
CNTNAP2 (isoform 1)	Isoform 1 of contactin-associated protein-like 2 (Caspr2 isoform 1)	2.8E+03	9.9E+02	9.8E+02	1.5E+05	1.6E+04	1.1E+05
ADAM22	Disintegrin and metalloproteinase domain-containing protein 22	5.4E+05	1.9E+05	6.8E+05	9.4E+06	1.2E+06	2.1E+06
KCNA1	Potassium voltage-gated channel subfamily A member 1 (Kv1.1)	2.3E+04	8.1E+03	2.6E+05	2.7E+07	1.5E+07	2.6E+07
DLG4	Disks large homolog 4	1.4E+05	4.2E+04	1.1E+07	4.6E+07	1.7E+06	5.4E+06

The IP replicates were performed and labeled as ADAM22_IP1; ADAM22_IP2, DLG4_IP1 and DLG4_IP2; and Kv1.1_IP1 and Kv1.1_IP2. The iBAQ values of the identified proteins are shown, corresponding to their protein abundance.

Table 3
Proteins identified from the IPs with anti-Caspr2 antibody from cortex extract.

Gene name	Protein name	KO1	KO2	WT1	WT2
CNTNAP2 (isoform 1)	Isoform 1 of contactin-associated protein-like 2 (Caspr2 isoform 1)	6.0E+03		6.1E+06	3.9E+07
CNTNAP2 (isoform 2)	Isoform 2 of contactin-associated protein-like 2 (Caspr2 isoform 2)	1.5E+06	2.0E+06	1.0E+06	1.0E+06
CNTN2	Contactin-2			1.0E+06	8.2E+06
ADAM11	Disintegrin and metalloproteinase domain-containing protein 11			2.2E+04	7.3E+05
ADAM22	Disintegrin and metalloproteinase domain-containing protein 22	1.7E+04	3.3E+03	1.2E+05	3.1E+06
ADAM23	Disintegrin and metalloproteinase domain-containing protein 23			5.5E+04	1.7E+06
DLG1	Disks large homolog 1			1.1E+05	7.2E+05
DLG2	Disks large homolog 2				8.8E+04
DLG4	Disks large homolog 4		2.0E+04	4.5E+04	1.3E+06
KCNAB1	Voltage-gated potassium channel subunit beta-1			1.1E+04	5.4E+04
KCNAB2	Voltage-gated potassium channel subunit beta-2	4.5E+04	4.7E+04	5.3E+05	2.4E+06
KCNA1	Potassium voltage-gated channel subfamily A member 1 (Kv1.1)			1.0E+04	1.6E+06
KCNA2	Potassium voltage-gated channel subfamily A member 2 (Kv1.2)			5.3E+04	1.8E+06
KCNA3	Potassium voltage-gated channel subfamily A member 3 (Kv1.3)				3.0E+05
KCNA4	Potassium voltage-gated channel subfamily A member 4 (Kv1.4)				3.4E+05
KCNA6	Potassium voltage-gated channel subfamily A member 6 (Kv1.6)			8.7E+04	2.0E+05
LGI1	Leucine-rich glioma-inactivated protein 1			6.5E+06	9.9E+06
LGI2	Leucine-rich glioma-inactivated protein 2			2.0E+03	5.4E+05
LGI3	Leucine-rich glioma-inactivated protein 3			1.0E+05	2.9E+05
LGI4	Leucine-rich glioma-inactivated protein 4			2.2E+04	6.2E+04
MPP2	MAGUK p55 subfamily member 2			2.8E+04	8.3E+04
MPP3	MAGUK p55 subfamily member 3		2.0E+03	1.9E+03	3.9E+05
CKMT1	Creatine kinase U-type, mitochondrial	5.0E+04	5.2E+04	4.8E+04	3.1E+04
CLU	Clusterin			9.9E+03	9.4E+04
PSME3	Proteasome activator complex subunit 3	1.0E+06	4.4E+05		
TPI1	Triosephosphateisomerase	4.5E+04	1.5E+05	1.1E+05	1.2E+05

The iBAQ values of the identified proteins are shown, corresponding to their protein abundance. When no values are depicted, signal was below detection limit. When no values are depicted, signal was below detection limit.

are consistently detected in the IPs of WT samples. An unexpected result is the presence of a Caspr2 variant in the KO samples, albeit at >10-fold lower amount. This short isoform 2 corresponds to the C-terminal region of the canonical Caspr2 isoform 1 and is distinguished from isoform1 by a single peptide that is cleaved differently by trypsin (Supplementary Fig. 1). ADAM22 and LGI1, and to a lesser extent the Kv1 channel, are also detected indicating that the isoform 2 is capable of interacting with a subset of the typical Caspr2 interactors.

Reverse IPs were performed on ADAM22, DLG4 and KCNA1 (Table 2). We confirmed the interaction of ADAM22, DLG4 and KCNA1 to Caspr2 isoform 1. However, we were not able to detect the short isoform 2 of Caspr2. The intensities of Caspr2 are generally low and close to the detection limit. Thus, it is likely that the lower expressed Caspr2 isoform 2 may exist in the protein complex at a level below the detection limit of our measurement.

We asked whether the isoform 2 is present solely in hippocampus and whether the use of detergent might affect the protein-protein interaction. We repeated the IP experiments using cortex as input and DDM for extraction and focused on proteins that were identified as Caspr2 interactors from hippocampus samples. Members of proteins identified in hippocampal IPs (Table 1) were also recovered in the cortex IPs (Table 3). MPPs and CLU were identified as Caspr2 interactors in both hippocampal and cortical samples. This strongly argues that they are the true interactors. Future experiments are needed to validate these interactions and their roles on Caspr2 function.

To further confirm the identity of isoform 2, we re-analyzed the IP data of the five SDS–PAGE gel slices. Fig. 4 shows that in WT sample,

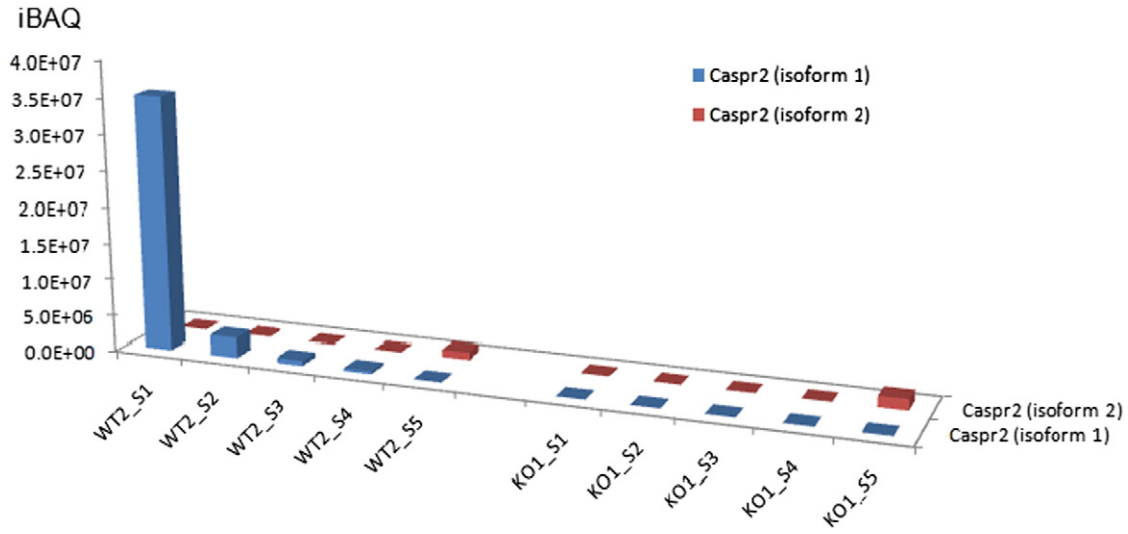

Fig. 4. The distribution ofCaspr2 isoforms 1 and 2 across the SDS–PAGE gel fractions. *x*-axis, SDS–PAGE gel slices number 1–5 (S1 – S2) corresponding from high to low masses from wild-type (WT) and knock out (KO) mice samples; *y*-axis, iBAQ values (see Table 3).

Caspr2 isoform 1 is present predominantly in gel slice 1 corresponding to the mass of > 100 kDa, whereas isoform 2 is present in gel slice 5 corresponding to mass <25 kDa. In the KO, Caspr2 isoform 2 is present in slice 5. The levels of Caspr2 isoform 2 in KO and WT are similar.

4. Discussion

Although Caspr2 has been associated genetically with ASD [8–10], its mechanistic contribution to autism is presently unknown. In this study, we aimed to identify the interacting proteins of Caspr2 and to establish the protein complexes, as a first step towards its functional analysis. We confirmed the expression of Caspr2 in juvenile and adult mice and its presence within and outside the synapse. Multiple interacting proteins of Caspr2 were revealed in this study. Moreover, we showed by studying knockout mice the existence of a short form of Caspr2 lacking most of the extracellular domains.

Caspr2 is known to play a critical role in the association of neurons and oligodendrocytes and in action potential propagation at the nodes of Ranvier of myelinated axons [13]. Caspr2 interacts with CNTN2 to form axon–glial contacts at the juxta-paranodes [12]. This adhesion complex enables the clustering of Kv1 channels, and the accumulation of scaffolding proteins, the MAGUKs DLG4 and DLG1 [13]. Recent pull-down experiments using the cytoplasmic domain of Caspr2 revealed the potential interaction of Caspr2 with another family of MAGUKs, the MPPs [13]. It was further suggested that the binding of protein 4.1 to Caspr2 allows the recruitment of MPPs to Caspr2 protein complex, but the in vivo evidence of Caspr2-MPP(s) interaction remained to be demonstrated [13]. The Caspr2 interacting Kv1 channels are responsible for the modulation of the action potential in the juxta-paranodes of the myelinated axons [11,12]. It was demonstrated that ADAM22 is an axonal component of the Kv1 channels and recruits MAGUKs to the juxta-paranodes [19]. However, ADAM22 is not essential for the clustering of Kv1 channels and Caspr2. Caspr2 is also abundantly present in the axon initial segment. It was suggested that the components of the Caspr2 protein complex in juxta-paranodes and axon initial segment are similar, but that the mechanism of protein clustering may differ. Taken together, based on literature data, the Caspr2 protein complex most likely contains CNTN2, and the Kv1 channels with its interactors, including different MAGUKs and ADAM22.

In the present study, we have carried out a comprehensive interaction proteomics analysis to reveal the Caspr2 interactome. We recovered the established Caspr2 interactors. Reverse IPs on ADAM22, DLG4 and KCNA1 further confirmed their interactions with Caspr2. However, Caspr2 interactome appears to be more complex than previously described. First, multiple members of the reported Caspr2 interactors may be contained in the Caspr2 complex. For example, three members of the ADAM family (ADAM11, ADAM22 and ADAM23), three members of the DLG family (DLG1, DLG2 and DLG4) and 4 members of the LGI family (LGI1, LGI2, LGI3 and LGI4) were identified in at least some of the Caspr2 IPs. This raises the possibility that different members of a family may be present in the same Caspr2 protein complex; alternatively, they may be mutual exclusively present in a Caspr2 protein complex. Second, the probable interaction between MPP and Caspr2 implicated from previous pull-down experiments is confirmed by the present study. Third, we detected novel Caspr2 interactors, such as CLU.

We further detected the presence of a short isoform 2 Caspr2. It was proposed that a short form comprising the C-terminal region (amino acids 1225 to 1332) of the full length Caspr2 exists [20,21]. Indeed, the identified Caspr2 peptides from the knockout sample all matched to this C-terminus of the full length Caspr2, thereby demonstrating the presence of the short form Caspr2 sequence. This short form of Caspr2 containing the full intracellular domain is capable of interacting with ADAM22, LGI1 and Kv1 channels, albeit at a lower level. This finding is in line with a previous study showing the requirement of the cytoplasmic domain of Caspr2 for Kv1 channel clustering. In contrast to this, the major Caspr2 interactor, CNTN2, does not interact with short form Caspr2, indicating the importance of the extracellular domains for the Caspr2-CNTN2 interaction. Given the specific loss of CNTN2 interaction, the short form Caspr2 might play role in the modulation of action potential propagation but should not contribute to cell-cell contact. Of notice is that the Caspr2 isoform 2 is also predicted to be present in human.

5. Conclusions

In conclusion, we characterized the composition of Caspr2 protein complex by interaction proteomics and revealed multiple interacting proteins including CNTN2, ADAM family, LGI1, Kv1 channels and MAGUKs. Furthermore, we demonstrated that Caspr2 isoform-specific complexes exist, which might provide relavance for the further dissection of dysfunctional molecular mechanisms underlying autism.

Supplementary data to this article can be found online at http://dx.doi.org/10.1016/j.bbapap.2015.02.008.

Transparency document

The Transparency document associated with this article can be found, in the online version.

Acknowledgement

Ning Chen was funded by a grant from the Netherlands Institute for Systems Biology (NISB (NWO-ALW)). Aaron Gordon and Elior Peles received support from the NIH (NS50220 to EP) and the Israel Science Foundation. Ka Wan Li, Roel C. van der Schors and August B. Smit received support from HEALTH-2009-2.1.2-1 EU-FP7 'SynSys' (#242167). Frank Koopmans was funded from the Netherlands Organization for Scientific Research (NWO) Complexity project 645.000.003.

References

[1] A.P. Association, The Fifth Edition of the Diagnostic and Statistical Manual of Mental Disorders (DSM-5), 2013 (Washington, DC).
[2] A. Ronald, E. Simonoff, J. Kuntsi, P. Asherson, R. Plomin, Evidence for overlapping genetic influences on autistic and ADHD behaviours in a community twin sample, J. Child Psychol. Psychiatry allied Discip. 49 (2008) 535–542.
[3] G.M. Anderson, Twin studies in autism: what might they say about genetic and environmental influences, J. Autism Dev. Disord. 42 (2012) 1526–1527.
[4] R.K. Yuen, B. Thiruvahindrapuram, D. Merico, S. Walker, K. Tammimies, N. Hoang, C. Chrysler, T. Nalpathamkalam, G. Pellecchia, Y. Liu, M.J. Gazzellone, L. D'Abate, E. Deneault, J.L. Howe, R.S. Liu, A. Thompson, M. Zarrei, M. Uddin, C.R. Marshall, R.H. Ring, L. Zwaigenbaum, P.N. Ray, R. Weksberg, M.T. Carter, B.A. Fernandez, W. Roberts, P. Szatmari, S.W. Scherer, Whole-genome sequencing of quartet families with autism spectrum disorder, Nat. Med. 21 (2015) 185–191.
[5] R. Holt, A.P. Monaco, Links between genetics and pathophysiology in the autism spectrum disorders, EMBO Mol. Med. 3 (2011) 438–450.
[6] M.W. State, P. Levitt, The conundrums of understanding genetic risks for autism spectrum disorders, Nat. Neurosci. 14 (2011) 1499–1506.
[7] C. Betancur, T. Sakurai, J.D. Buxbaum, The emerging role of synaptic cell-adhesion pathways in the pathogenesis of autism spectrum disorders, Trends Neurosci. 32 (2009) 402–412.
[8] O. Penagarikano, B.S. Abrahams, E.I. Herman, K.D. Winden, A. Gdalyahu, H. Dong, L.I. Sonnenblick, R. Gruver, J. Almajano, A. Bragin, P. Golshani, J.T. Trachtenberg, E. Peles, D.H. Geschwind, Absence of CNTNAP2 leads to epilepsy, neuronal migration abnormalities, and core autism-related deficits, Cell 147 (2011) 235–246.
[9] O. Penagarikano, D.H. Geschwind, What does CNTNAP2 reveal about autism spectrum disorder? Trends Mol. Med. 18 (2012) 156–163.
[10] G.R. Anderson, T. Galfin, W. Xu, J. Aoto, R.C. Malenka, T.C. Sudhof, Candidate autism gene screen identifies critical role for cell-adhesion molecule CASPR2 in dendritic arborization and spine development, Proc. Natl. Acad. Sci. U. S. A. 109 (2012) 18120–18125.
[11] S. Poliak, D. Salomon, H. Elhanany, H. Sabanay, B. Kiernan, L. Pevny, C.L. Stewart, X. Xu, S.Y. Chiu, P. Shrager, A.J. Furley, E. Peles, Juxtaparanodal clustering of Shaker-like K+ channels in myelinated axons depends on Caspr2 and TAG-1, J. Cell Biol. 162 (2003) 1149–1160.
[12] M. Traka, L. Goutebroze, N. Denisenko, M. Bessa, A. Nifli, S. Havaki, Y. Iwakura, F. Fukamauchi, K. Watanabe, B. Soliven, J.A. Girault, D. Karagogeos, Association of TAG-1 with Caspr2 is essential for the molecular organization of juxtaparanodal regions of myelinated fibers, J. Cell Biol. 162 (2003) 1161–1172.
[13] I. Horresh, S. Poliak, S. Grant, D. Bredt, M.N. Rasband, E. Peles, Multiple molecular interactions determine the clustering of Caspr2 and Kv1 channels in myelinated axons, J. Neurosci. Off. J. Soc. Neurosci. 28 (2008) 14213–14222.

[14] M.C. Inda, J. DeFelipe, A. Munoz, Voltage-gated ion channels in the axon initial segment of human cortical pyramidal cells and their relationship with chandelier cells, Proc. Natl. Acad. Sci. U. S. A. 103 (2006) 2920–2925.
[15] B. Bakkaloglu, B.J. O'Roak, A. Louvi, A.R. Gupta, J.F. Abelson, T.M. Morgan, K. Chawarska, A. Klin, A.G. Ercan-Sencicek, A.A. Stillman, G. Tanriover, B.S. Abrahams, J.A. Duvall, E.M. Robbins, D.H. Geschwind, T. Biederer, M. Gunel, R.P. Lifton, M.W. State, Molecular cytogenetic analysis and resequencing of contactin associated protein-like 2 in autism spectrum disorders, Am. J. Hum. Genet. 82 (2008) 165–173.
[16] S. Spijker, Dissection of rodent brain regions, in: K.W. Li (Ed.), Neuroproteomics, Humana Press, New York, Dordrecht, Heidelberg, London, 2011, pp. 13–26.
[17] K.W. Li, N. Chen, P. Klemmer, F. Koopmans, R. Karupothula, A.B. Smit, Identifying true protein complex constituents in interaction proteomics: the example of the DMXL2 protein complex, Proteomics 12 (2012) 2428–2432.
[18] N. Chen, R.C. van der Schors, A.B. Smit, A 1D-PAGE/LC-ESI Linear Ion Trap Orbitrap MS Approach for the Analysis of Synapse Proteomes and Synaptic Protein Complexes, in: K.W. Li (Ed.), Neuroproteomics, Humana Press, New York, Dordrecht, Heidelberg, London, 2011, pp. 159–168.
[19] Y. Ogawa, J. Oses-Prieto, M.Y. Kim, I. Horresh, E. Peles, A.L. Burlingame, J.S. Trimmer, D. Meijer, M.N. Rasband, ADAM22, a Kv1 channel-interacting protein, recruits membrane-associated guanylate kinases to juxtaparanodes of myelinated axons, J. Neurosci. Off. J. Soc. Neurosci. 30 (2010) 1038–1048.
[20] P. Carninci, T. Kasukawa, S. Katayama, J. Gough, M.C. Frith, N. Maeda, R. Oyama, T. Ravasi, B. Lenhard, C. Wells, R. Kodzius, K. Shimokawa, V.B. Bajic, S.E. Brenner, S. Batalov, A.R. Forrest, M. Zavolan, M.J. Davis, L.G. Wilming, V. Aidinis, J.E. Allen, A. Ambesi-Impiombato, R. Apweiler, R.N. Aturaliya, T.L. Bailey, M. Bansal, L. Baxter, K.W. Beisel, T. Bersano, H. Bono, A.M. Chalk, K.P. Chiu, V. Choudhary, A. Christoffels, D.R. Clutterbuck, M.L. Crowe, E. Dalla, B.P. Dalrymple, B. de Bono, G. Della Gatta, D. di Bernardo, T. Down, P. Engstrom, M. Fagiolini, G. Faulkner, C.F. Fletcher, T. Fukushima, M. Furuno, S. Futaki, M. Gariboldi, P. Georgii-Hemming, T.R. Gingeras, T. Gojobori, R.E. Green, S. Gustincich, M. Harbers, Y. Hayashi, T.K. Hensch, N. Hirokawa, D. Hill, L. Huminiecki, M. Iacono, K. Ikeo, A. Iwama, T. Ishikawa, M. Jakt, A. Kanapin, M. Katoh, Y. Kawasawa, J. Kelso, H. Kitamura, H. Kitano, G. Kollias, S.P. Krishnan, A. Kruger, S.K. Kummerfeld, I.V. Kurochkin, L.F. Lareau, D. Lazarevic, L. Lipovich, J. Liu, S. Liuni, S. McWilliam, M. Madan Babu, M. Madera, L. Marchionni, H. Matsuda, S. Matsuzawa, H. Miki, F. Mignone, S. Miyake, K. Morris, S. Mottagui-Tabar, N. Mulder, N. Nakano, H. Nakauchi, P. Ng, R. Nilsson, S. Nishiguchi, S. Nishikawa, F. Nori, O. Ohara, Y. Okazaki, V. Orlando, K.C. Pang, W.J. Pavan, G. Pavesi, G. Pesole, N. Petrovsky, S. Piazza, J. Reed, J.F. Reid, B.Z. Ring, M. Ringwald, B. Rost, Y. Ruan, S.L. Salzberg, A. Sandelin, C. Schneider, C. Schonbach, K. Sekiguchi, C.A. Semple, S. Seno, L. Sessa, Y. Sheng, Y. Shibata, H. Shimada, K. Shimada, D. Silva, B. Sinclair, S. Sperling, E. Stupka, K. Sugiura, R. Sultana, Y. Takenaka, K. Taki, K. Tammoja, S.L. Tan, S. Tang, M.S. Taylor, J. Tegner, S.A. Teichmann, H.R. Ueda, E. van Nimwegen, R. Verardo, C.L. Wei, K. Yagi, H. Yamanishi, E. Zabarovsky, S. Zhu, A. Zimmer, W. Hide, C. Bult, S.M. Grimmond, R.D. Teasdale, E.T. Liu, V. Brusic, J. Quackenbush, C. Wahlestedt, J.S. Mattick, D.A. Hume, C. Kai, D. Sasaki, Y. Tomaru, S. Fukuda, M. Kanamori-Katayama, M. Suzuki, J. Aoki, T. Arakawa, J. Iida, K. Imamura, M. Itoh, T. Kato, H. Kawaji, N. Kawagashira, T. Kawashima, M. Kojima, S. Kondo, H. Konno, K. Nakano, N. Ninomiya, T. Nishio, M. Okada, C. Plessy, K. Shibata, T. Shiraki, S. Suzuki, M. Tagami, K. Waki, A. Watahiki, Y. Okamura-Oho, H. Suzuki, J. Kawai, Y. Hayashizaki, F. Consortium, R.G.E.R. Group, G. Genome Science, The transcriptional landscape of the mammalian genome, Science 309 (2005) 1559–1563.
[21] D.S. Gerhard, L. Wagner, E.A. Feingold, C.M. Shenmen, L.H. Grouse, G. Schuler, S.L. Klein, S. Old, R. Rasooly, P. Good, M. Guyer, A.M. Peck, J.G. Derge, D. Lipman, F.S. Collins, W. Jang, S. Sherry, M. Feolo, L. Misquitta, E. Lee, K. Rotmistrovsky, S.F. Greenhut, C.F. Schaefer, K. Buetow, T.I. Bonner, D. Haussler, J. Kent, M. Kiekhaus, T. Furey, M. Brent, C. Prange, K. Schreiber, N. Shapiro, N.K. Bhat, R.F. Hopkins, F. Hsie, T. Driscoll, M.B. Soares, T.L. Casavant, T.E. Scheetz, M.J. Brown-stein, T.B. Usdin, S. Toshiyuki, P. Carninci, Y. Piao, D.B. Dudekula, M.S. Ko, K. Kawakami, Y. Suzuki, S. Sugano, C.E. Gruber, M.R. Smith, B. Simmons, T. Moore, R. Waterman, S.L. Johnson, Y. Ruan, C.L. Wei, S. Mathavan, P.H. Gunaratne, J. Wu, A.M. Garcia, S.W. Hulyk, E. Fuh, Y. Yuan, A. Sneed, C. Kowis, A. Hodgson, D.M. Muzny, J. McPherson, R.A. Gibbs, J. Fahey, E. Helton, M. Ketteman, A. Madan, S. Rodrigues, A. Sanchez, M. Whiting, A. Madari, A.C. Young, K.D. Wetherby, S.J. Granite, P.N. Kwong, C.P. Brinkley, R.L. Pearson, G.G. Bouffard, R.W. Blakesly, E.D. Green, M.C. Dickson, A.C. Rodriguez, J. Grimwood, J. Schmutz, R.M. Myers, Y.S. Butterfield, M. Griffith, O.L. Griffith, M.I. Krzywinski, N. Liao, R. Morin, D. Palmquist, A.S. Petrescu, U. Skalska, D.E. Smailus, J.M. Stott, A. Schnerch, J.E. Schein, S.J. Jones, R.A. Holt, A. Baross, M.A. Marra, S. Clifton, K.A. Makowski, S. Bosak, J. Malek, M.G.C.P. Team, The status, quality, and expansion of the NIH full-length cDNA project: the Mammalian Gene Collection (MGC), Genome Res. 14 (2004) 2121–2127.